Recent Development of LS-DYNA® XFEM Shells for Dynamic Ductile Failure Analysis: XFEM with GISSMO Damage Model

Y. Guo*, C. T. Wu
Livermore Software Technology (LST), an ANSYS company
7374 Las Positas Road, Livermore, CA 94551, USA

Abstract

This paper presents a coupling of LS-DYNA XFEM shell method [30] and GISSMO damage model for dynamic ductile failure in shell structures. The XFEM shell formulation adopts the finite element continuous-discontinuous approach with the phantom-node technique [17] employed to incorporate velocity discontinuities in standard shell finite element formulations. The generalized incremental stress-state dependent damage model (GISSMO) adds damage and failure to most material models in LS-DYNA that do not allow failure. With the stress-triaxiality dependent failure criterion provided in GISSMO model, XFEM can better simulate material failure and crack propagation in mixed modes and under more complicated loading conditions. The option of element-size dependent regularization factor in GISSMO model removes the strain localization existing in the standard continuum damage model and suppresses the element-size sensitivity of ductile fracture, which is similar to the regularization zone approach in our original XFEM shell method for ductile fracture [30-32]. Unlike element erosion, when an element fails after certain number of integration points reach failure criterion, a crack (discontinuity)is inserted into the element with its direction depending on the stress state or other propagation option, and the element becomes an XFEM element comprised of two phantom elements. XFEM formulation allows crack propagation across elements without the sensitivity on mesh discretization and maintains the conservations of mass and momentum. Several numerical benchmarks and examples are tested using the explicit dynamics analysis to demonstrate the effectiveness and accuracy of the method described in this paper.

1. Introduction

Failure and fracture analyses in metal materials are increasingly important in many industries. For the automotive industry, lightweight materials such as the high-strength steel have a direct impact on driving dynamics, fuel consumption and agility. While the structure made of high-strength steel offers superior stiffness with reduced weight, material failure analysis in high-strength steel structure becomes critical for crashworthiness simulation in modern lightweight vehicle design. In contrast to brittle fracture in concretes and rocks, the ductile failure in metals undergoes a certain amount of plastic deformation before a macro-crack is evident. Microscopically, this ductile damage phenomenon is associated with voids nucleation, growth and coalescence under high and moderate stress triaxiality [1]. Macroscopically, the ductile damage is represented by the progressive degradation of material as a consequence of the growth of microstructural defects and can be modeled phenomenologically using the continuum damage mechanics [2,3]. When the coalescence of some microstructural defects creates the macro-crack, the discrete fracture becomes dominant as the ultimate result of the material degradation process [3] in ductile fracture.

Standard numerical simulations using the continuum damage models are known to be susceptible to the pathological localization of deformation. To regularize the non-unique solution in damage-induced strain localization problems, several integral-type and gradient-type of nonlocal damage models [4-6] and phase field model [7] based on regularized variational formulation were developed.

When the coalescence of some microstructural defects creates the macro-crack, the discrete fracture becomes dominant and rupture occurs in ductile materials. Unfortunately, the numerical methods based on a pure nonlocal damage model are inadequate to describe such kinematic discontinuity of the displacement field in a

continuous setting [8]. To release the excessive straining in the damage zone and achieve a better representation of the entire failure process, many combined continuous-discontinuous approaches [8,9,10-13] have been developed. While the nonlocal damage model is used to describe the material degradation, the discontinuous enrichment [14-16] typically used in fracture mechanics are usually considered to model the discrete crack. Among those discontinuous enrichment methods, the phantom-node approach [17] in extended finite element method (XFEM) [18, 19] is attractive to model the ductile fracture in plate and shell structures. The phantom-node approach describes a crack with two standard overlapping elements, therefore, it can be directly applied to any existing finite element code, for example, the 4-noded element using a fully integrated shear deformable shell formulation [21, 22].

While there are several constitutive models with continuum damage mechanics in LS-DYNA, many material laws for metallic materials do not allow damage failure. The generalized incremental stress-state dependent damage model (GISSMO) [22] provides an easy way to add continuum damage mechanics to any constitutive models for ductile materials. Its failure criterion can be function of stress state, making it suitable for simulation of ductile fracture in mixed modes. The GISSMO model also has an option of element-size dependent regularization factor, which can be used to minimize the strain localization problem in ductile fracture. Although GISSMO model is a phenomenological constitutive law and its parameters need many experiments and numerical calibrations to obtain, we think it is worth of adding GISSMO damage model in LS-DYNA XFEM formulations for ductile fracture.

In this paper, we present LS-DYNA XFEM shell formulations for ductile fracture using GISSMO damage model as failure criterion. The rest of the paper is organized as follows: Section 2 briefly summaries the XFEM shell formulations in LS-DYNA and provides the computational flow and keyword format to use XFEM. Section 3 describes the keywords for GISSMO damage model. Three numerical examples are given in Section 4, and finally the conclusions are made in Section 5.

2. LS-DYNA XFEM Shell Formulations

The XFEM phantom-node approach has been applied to three finite element shell formulations in LS-DYNA, the one-point integrated Belytschko-Lin-Tsay shell with hourglass control [23], the four-node fully integrated shear deformable shell formulation [21, 22] with assumed strain interpolants [24, 25] for alleviating the shear locking and for enhancing the in-plane bending behavior, and recently the discrete Kirchoff triangular element [22]. Through-the-thickness, element-wise discontinuous velocity and angular velocity fields are introduced to the standard shell element formulation using the XFEM phantom-node approach to model the internal discontinuity in a shell element when fracture occurs in this element.

Unlike the brittle fracture where material failure is controlled by stress-based criterion, such as the maximum tensile strength in Mode-I fracture, the ductile failure is determined by strain-based criterion. With a standard plastic constitutive model, the transition from continuous to discontinuous state can be triggered when a critical plastic strain threshold is reached. In this case, a modified cohesive zone model is applied to the newly activated crack surface to account for the energy released from the crack surface. With the continuum damage model, the transition from damage to crack is triggered when the material is fully degraded. In this scenario, a traction-free crack [15,20] is introduced to the numerical model as the damage variable is close to one. These local material models cannot be directly used for numerical simulations of ductile fracture, nonlocal processing procedure needs to be applied to remove the mesh sensitivity problem. The regularization of the failure strain or the effective plastic strain are proposed and implemented in LS-DYNA [30-32].

Detailed theories on these element formulations and phantom-node XFEM can be found in relevant literatures and are omitted in this paper.

2.1 Computational flow chart

The computational procedure of the phantom-node XFEM is given in the following.

1. Check crack initiation/propagation.
   1.1 Compute non-local effective plastic strain in candidate elements.
   1.2 Compute damage variable if continuous damage model is used.
   1.3 If damage variable exceeds critical value, or effective plastic strain reaches criterion, active XFEM.
      1.3.1 For crack initiation, crack direction determined by first principal strain; for crack propagation, crack direction determined by damage/plastic strain center. Calculate crack line in the element in initial configuration.
      1.3.2 Add phantom nodes; replace the original shell element with two overlapping phantom elements which are comprised of real nodes and phantom nodes but have same element formulation as the replaced element.
      1.3.3 Calculate lumped mass for added phantom nodes and update lumped mass for the real nodes.
      1.3.4 Constrain the phantom nodes on the crack tip edge.
2. Update kinetical variables on real nodes and phantom nodes if any.
3. Advance one time-step.
   3.1 Set nodal forces to zero.
   3.2 Apply external load, including contact force.
4. Loop through regular finite elements and phantom elements.
   4.1 Calculate strain rate at Gauss points. Update strain components.
   4.2 Update stress components using continuous damage constitutive law.
   4.3 Calculate nodal forces at real nodes for all elements, and phantom nodes if it's a phantom element.
   4.4 If in a regular element the damage variable/effective plastic strain at any Gauss point exceeds the critical value, mark this element as an XFEM candidate.
5. Go to 1.

2.2 Keyword for XFEM shells

XFEM shells can be activated using keyword *SECTION_SHELL. The keyword format is as follows

***SECTION_SHELL_{XFEM}**

Card 1	1	2	3	4	5	6	7	8
Variable	SECID	ELFORM	SHRF	NIP	PROPT	QR/IRID	ICOMP	SETYP
Type	I	I	F	I	F	F	I	I

Card 3	1	2	3	4	5	6	7	8
Variable	MCID	BASELM	DOMINT	FAILCR	PROPCR	FS	LS/FS1	NC/LC
Type	I	I	I	I	I	F	F	F

ELFORM = 52 for 2D plain strain
= 54 for shell
MCID: Material ID for cohesive law
BASELM = 2 for base shell element type 2 (default for shell) = 13 for 2D plain strain (default for 2D)
= 16 for base shell element type 16
= 17 for DKT shell element type 17
DOMINT: Option for domain integration for XFEM
= 0 phantom element integration (default)
= 1 subdomain integration (not available in shell XFEM)
FAILCR: Failure criterion
= 0 GISSMO damage model
= 1 maximum tensile strength (value given in cohesive law)
= -1 critical effective plastic strain
= -2 crack length dependent EPS
= -3 continuum damage model
PROPCR: Option for crack propagation direction
= 0 first principal total strain direction
= 2 center of effective plastic strain
= 3 damage center
FS: Failure strain/Failure critical value
LS: Length scale for strain regularization, >0 actives strain regularization, available for FAILCR=-1
NC: Number of cracks allowed. NC<0 (or NC=-99) activates element erosion for failed XFEM elements.
When FAILCR=-2, a crack-length dependent critical effective plastic strain is defined as

$$\varepsilon_{crit} = \varepsilon_0 - \min(1.0,\ l / l_c) * (\varepsilon_0 - \varepsilon_1) \quad (1)$$

where ε_0 is initial failure plastic strain FS, ε_1 is final failure plastic strain FS1, l_c is crack length LC at final plastic strain and l is crack length.

3. GISSMO Damage Model

With continuum damage models or standard plastic constitutive models, the finite element simulations using local failure criterion are susceptable to the mesh sensitivity problem. To avoid the pathological localization of deformation and damage growth in XFEM shell computation, the integral-type of nonlocal modeling [4] is adopted in LS-DYNA XFEM shell formulation for ductile fracture [30-32]. However, there are many material laws in LS-DYNA that do not allow damage and failure. To remedy this drawback, GISSMO damage model has been implemented in LS-DYNA by DYNAmore. Activating GISSMO model for XFEM failure criterion is a natural way to access the vast library of material laws in the form of continuum damage model.

3.1 Keywords for GISSMO damage model

In LS-DYNA, there are two keywords to add the GISSMO damage model to any material laws that do not have damage failure: the old keyword *MAT_ADD_EROSION and new keyword *MAT_ADD_DAMAGE_GISSMO. We will briefly describe the two keywords in this section and the theory and details of all the parameters can be found in the relevant literatures and LS-DYNA material manual.

*MAT_ADD_EROSION

Card 1	1	2	3	4	5	6	7	8
Variable	MID	EXCL	MXPRES	MNEPS	EFFEPS	VOLEPS	NUMFIP	NCS
Type	A8	F	F	F	F	F	F	F
Card 3	1	2	3	4	5	6	7	8
Variable	IDAM	DMGTYP	LCSDG	ECRIT	DMGEXP	DCRIT	FADEXP	LCREGD
Type	I	F	I	F	F	F	F	F
Card 4	1	2	3	4	5	6	7	8
Variable	SIZFLG	REFSZ	NAHSV	LCSRS	SHRF	BIAXF		
Type	F	F	I	F	F	F		

*MAT_ADD_DAMAGE_GISSMO

Card 1	1	2	3	4	5	6	7	8
Variable	MID		DTYP	REFSZ	NUMFIP			
Type	A8		F	F	F			
Card 2	1	2	3	4	5	6	7	8
Variable	LCSDG	ECRIT	DMGEXP	DCRIT	FADEXP	LCREGD		
Type	F	F	I	F	F	F		
Card 3	1	2	3	4	5	6	7	8
Variable	LCSRS	SHRF	BIAXF	LCDLIM	MIDFAIL	HISVN		
Type	A8	F	I	F	F	F		

MID: Material identification for which this erosion definition applies.
IDAM: Flag for damage model (only in *MAT_ADD_EROSION)
= 1 for GISSMO damage model
LCSDG: Load curve ID or Table ID. Load curve defines equivalent plastic strain to failure vs. triaxiality. Table defines for each Lode parameter value (between -1 and 1) a load curve ID giving the equivalent plastic strain to failure vs. triaxiality for that Lode parameter value.
LCREGD: Load curve ID or Table ID defining element size dependent regularization factors for equivalent plastic strain to failure.

3.2 Stress-triaxiality dependent failure strain

Usually the failure of ductile materials occurs at different failure strain in different failure modes and the failure modes are defined by the stress state. This phenomenon can be described by the equivalent plastic strain at failure as a function of stress triaxiality. A typical stress-triaxiality dependent effective plastic strain at failure for shell structure can be demonstrated as the curve in Figure 1. From the curve, we can see the failure strain of ductile shell in tension mode is the smallest, followed by that of shear mode (stress triaxiality is zero) and the material is most difficult to fail in compression mode.

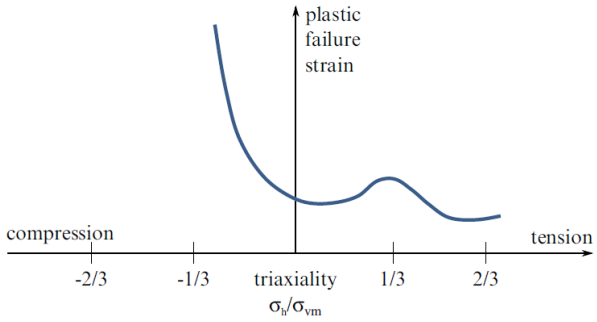

Figure 1. Typical failure curve for metal sheet, modeled with shell elements

4. Numerical examples

In this section, two benchmarks and one numerical example are analyzed to study the performance of present method in the shell fracture analysis. Unless otherwise specified, dimensionless unit system is adopted in this paper. Since we do not have the data of element-size dependent regularization factor for GISSMO model at the time of writing this paper, we will not test its performance at this time.

4.1 Tension coupon test

The first benchmark is the tension coupon test. The tension coupon is a rectangular plate of 203.2mm long by 44.45mm width and a thickness of 1.7272mm, with a reduced middle region of 25.4mm width, as shown in Figure 2. The left side of the coupon is fixed, and the right side is applied a pulling velocity gradually increasing from 0 to 0.1mm/ms at 1.0ms and remaining at the speed. The simulation time is 30ms. The material is steel with a density of 7.8×10^{-6} kg/mm^3, Young's modulus of 210GPa, Possion's ratio of 0.3 and nonlinear strain hardening curve (initial yield stress is 346MPa) and is modelled by *MAT_PIECEWISE_LINEAR_PLASTICITY. The GISSMO model has a stress triaxiality dependent failure strain similar as shown in Figure 1.

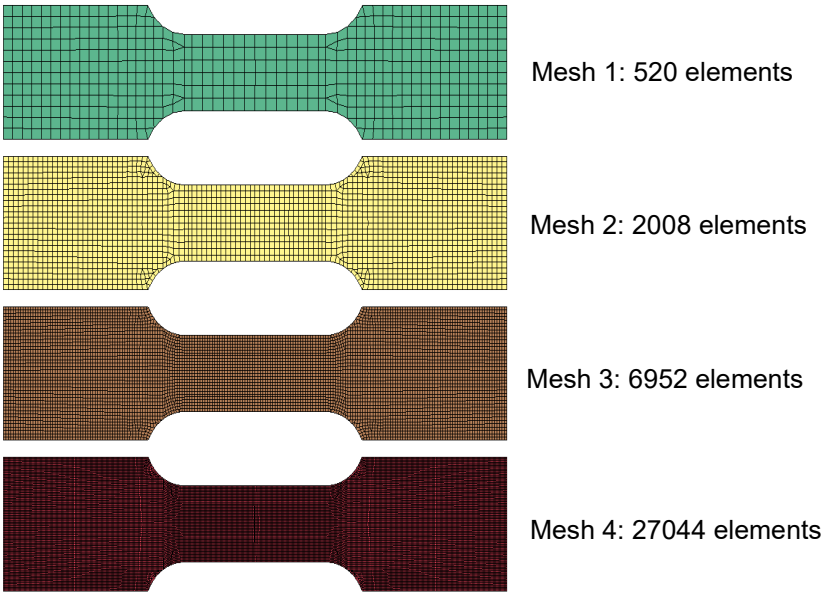

Figure 2. Four mesh refinements of the tension coupon

The coupon is discretized by four meshes with different numbers of elements, as shown in Figure 2. This tension coupon problem is solved by both FEM with element erosion and XFEM.

Both the FEM and XFEM give similar results in the deformation of the coupon. With the increased pulling, the coupon undergoes plastic deformation in the narrowed region and develops necking in the middle of the coupon. The crack initiates inside the coupon at the center and propagates vertically. Figure 3 shows the comparison of the section force histories obtained by the four meshes and two numerical methods. From the plots, we can see the solution seems to converge with the mesh refinement. Except for the result given by the coarsest mesh, Mesh 1, the force responses from the other three meshes are very close, indicating that the mesh size effect does not exist in this tension test, even though there is no element-size dependent regularization factor in the GISSMO model used in the simulation. The behavior is the same for both FEM and XFEM. The reason is that the crack initiates in the middle of the coupon, which is in a biaxial stress state. The biaxial stresses tend to be less sensitive to mesh-size effect, as long as the mesh is not too coarse.

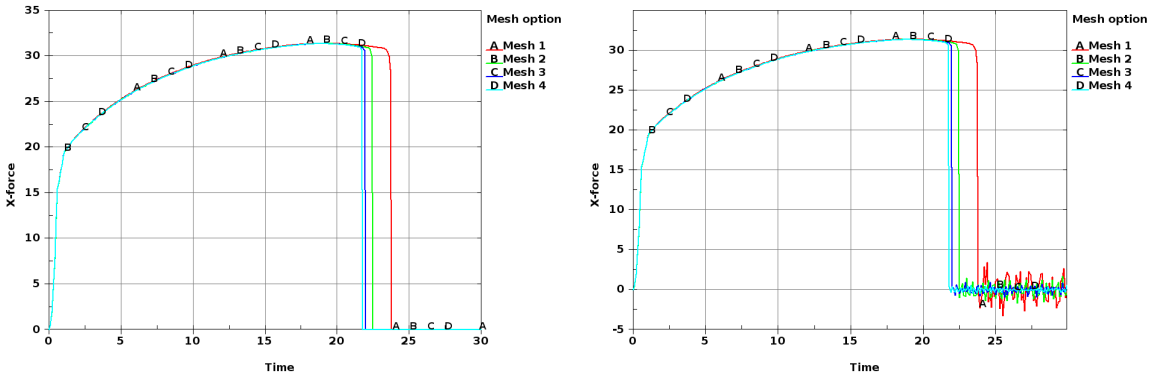

(a) FEM (b) XFEM

Figure 3. Comparison of section force histories

As to the crack pattern, both the FEM and XFEM give similar results too. The crack initiates at the center of the coupon and propagates vertically outwards to the upper and lower boundaries, resulting in a vertical crack in the

middle of the coupon. Figure 4 shows the crack patterns given by XFEM in both initial (undeformed) and final (deformed) configuration, which are very consistent across different mesh refinements.

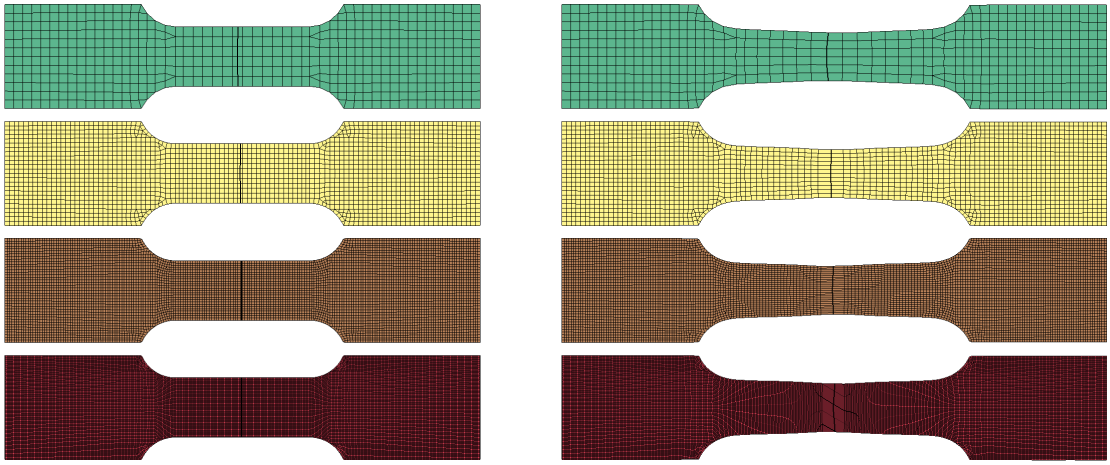

(a) Initial configuration (b) Final configuration

Figure 4. Crack patterns in initial and final configurations by XFEM

4.2 Shear coupon test

In the second benchmark, a shear coupon test is analyzed. The coupon with a length of 114.3mm and a width of 25.4mm has two U-shape notches at 45° deeply cut into the coupon as shown in Figure 5, resulting in a small region roughly represented by a rectangle of 4.9mm by 1.5mm (green region). When the coupon is applied uniaxial tensile loading, the green region will be in shear mode.

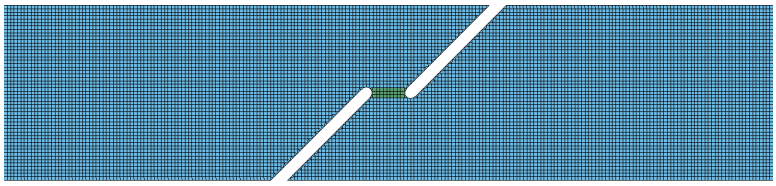

Figure 5. Shear coupon under stretching loading

The coupon is modelled by two parts. The small shear mode part consists of 31 elements and has a thickness of 1.3208mm. The rest of the coupon has a thickness of 1.7272mm and is discretized with 11478 elements. The left side of the coupon is fixed, and the right side is applied a pulling velocity gradually increasing from 0 to 0.1mm/ms at 1.0ms and remaining at the speed. The simulation time is 12ms. The material is steel with a density of 7.8×10^{-6}kg/mm^3, Young's modulus of 210GPa, Possion's ratio of 0.3 and nonlinear strain hardening curve (initial yield stress is 346MPa) and is modelled by *MAT_PIECEWISE_LINEAR_PLASTICITY. The GISSMO model has a stress triaxiality dependent failure strain as shown in Figure 1. This problem is solved by both FEM with element erosion and XFEM.

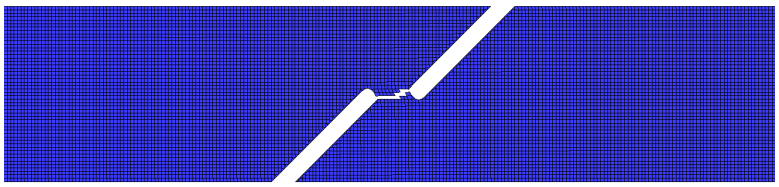

(a) FEM with Element Erosion

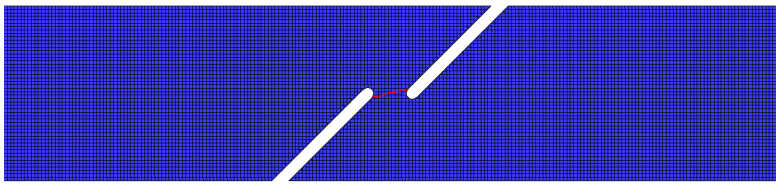

(b) XFEM

Figure 6. Crack patterns obtained by FEM and XFEM

The crack patterns given by FEM and XFEM for the shear coupon test are very similar, as shown in Figure 6. The cracks initiate at the tips of the U-shaped notches, propagate inwards and merge into one crack. The section forces obtained by FEM and XFEM are agreeable too, as shown in Figure 7.

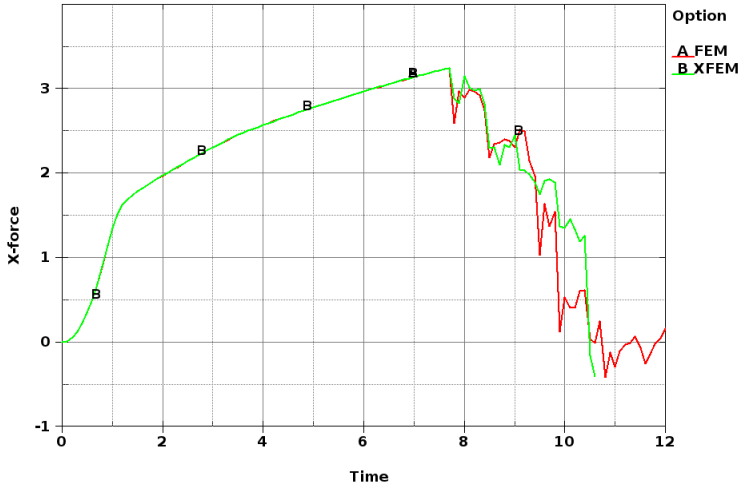

Figure 7. Comparison of section force histories by FEM and XFEM

4.3 Asymmetric V-notched specimen under tensile loading

In this numerical example, the fracture of an asymmetric V-notched specimen under tensile loading is studied. The model set up of the specimen is illustrated in Figure 8. The specimen has a length of 210mm, a width of 50mm and a thickness of 1.6mm. The two V-shaped notches with 90° opening are located 7mm away from the middle of the specimen separately, forming an angle of about 20° with the vertical line. The specimen is clamped on the left end (green region) and applied a pulling velocity of 10mm/ms at the right end (yellow region). The material of the specimen is steel with a density of 7.8×10^{-6}kg/mm^3, Young's modulus of 210GPa, Possion's ratio of 0.3 and nonlinear strain hardening curve (initial yield stress is 346MPa).

The specimen has a mesh discretization of 8878 elements, as shown in Figure 8. The material is modelled by *MAT_PIECEWISE_LINEAR_PLASTICITY. The GISSMO model has a stress triaxiality dependent failure strain as shown in Figure 1. This numerical example is solved by both FEM with element erosion and XFEM, with a simulation time of 1.0ms.

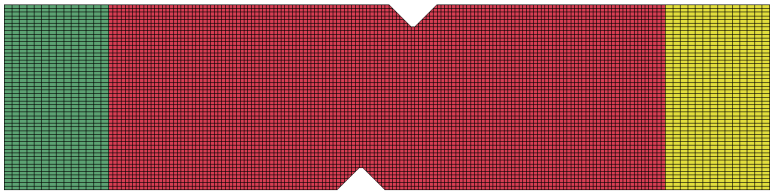

Figure 8. Asymmetric V-notched specimen under tensile loading

Figure 9 shows the crack patterns given by FEM and XFEM. We can see from the crack patterns that the fracture of the specimen is in mode I (tension mode) at the beginning stage, illustrated by the two vertical cracks originating from the V-shaped notches. Then the fracture mode changes to Mode II (shear mode) and the two vertical cracks merge into one crack. However, the crack patterns in shear mode given by FEM and XFEM are quite different. The shear crack given by FEM has an angle of about 10° while the shear crack given by XFEM has an angle close to 45° which agrees with experimental result. There are two reasons that the FEM yields erroneous result in shear mode: The first is that the element erosion changes the physical domain of the problem and the second is that the element erosion causes loss of conservations of mass and momentum. The difference between FEM and XFEM results also presents in the comparison of the section force histories as shown in Figure 10. FEM with element erosion underestimates the section force right after the cracks initiate.

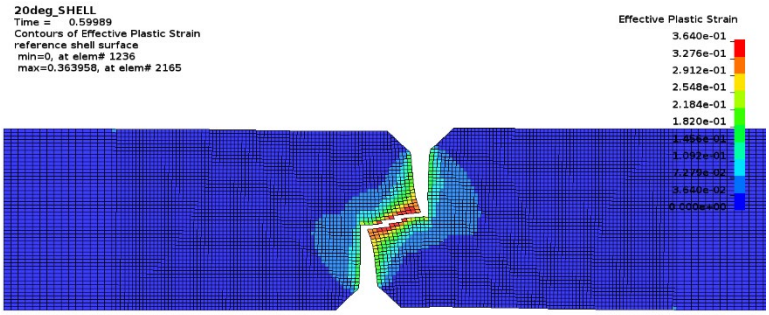

(a) FEM with Element Erosion

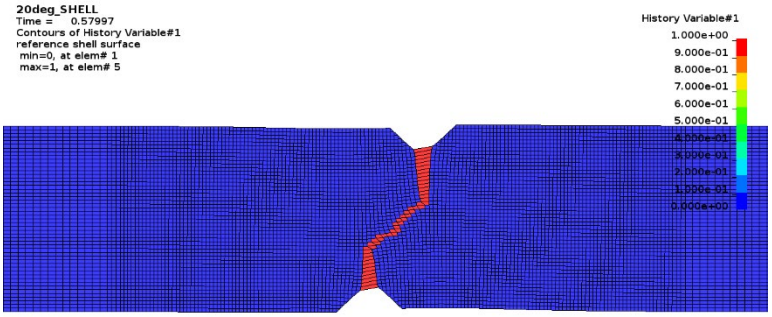

(b) XFEM

Figure 9. Crack patterns obtained by FEM and XFEM

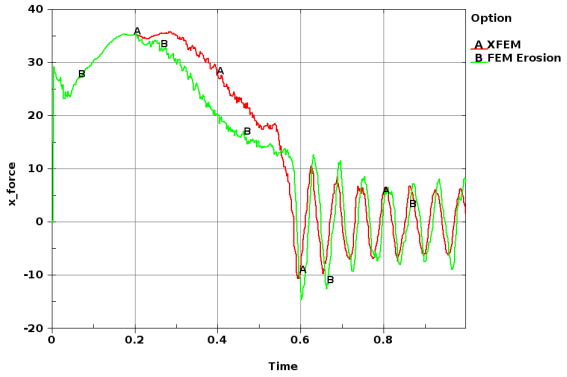

Figure 10. Comparison of section force histories

5. Conclusions

GISSMO damage model is added to LS-DYNA XFEM shell formulations for material failure and crack propagation in ductile metalic shell structures. GISSMO model not only provides continuum damage mechanics to a variety of constitutive models in LS-DYNA that do not have damage failure, its stress-triaxiality dependent failure criterion lets XFEM formulations better simulate ductile fracture in mixed modes and under more complicated loading conditions. The effectiveness of its element-size dependent regularization factor in suppressing strain localization problem in ductile failure waits to be investigated. The numerical results in this study indicate that LS-DYNA XFEM shell formulations with GISSMO damage model can simulate ductile fracture in different modes with ease and provides the way to access more constitutive models in the framework of continuum damage mechanics.

References

1. Tai HW (1990) Plastic damage and ductile fracture in mild steels. Engng Fract Mech 36:583-580
2. Chaboche JL (1988) Continuum damage mechanics. Part I: General Concepts, J Appl Mech 55:59-64
3. Lemaitre J, Chaboche JL (1990) Mechanics of Solid Materials. Cambridge University Press, Cambridge
4. Bažant ZP, Belytschko T, Chang TP (1984) Continuum theory for strain soften. J Engrg Mech 110:1666-1692
5. de Borst R, Muhlhaus HB (1992) Gradient-dependent plasticity: formulation and algorithm aspects. Int J Numer Methods Engrg 35:521-539
6. Chen JS, Wu CT, Belytschko T (2000) Regularization of material instabilities by meshfree approximations with intrinsic length scales. Int J Numer Methods Engrg 47:1303-1322
7. Doan DH, Bui TQ, Duc ND, Fushinobu K (2016) Hybrid phase field simulation of dynamic crack propagation in functionally graded glass-filled epoxy. Compos Part B: Eng 99:266-276
8. Seabra MRR, Cesar de Sa JMA, Andrade FXC, Pires FFMA (2011) Continuous-discontinuous formulation for ductile fracture. Int J Mater Form 4:271-281
9. Mediavilla J, Peerlings RHJ, Geers MGD (2006) A robust and consistent remeshing-transfer operator for ductile fracture simulations. Comput Structures 84:604-623
10. Mazars J, Pijaudier-Cabot G (1996) From damage to fracture mechanics and conversely: a combined approach. Int J Solid Struct 33:3327-3342
11. Oliver J, Huespe AE, Pulido MDG, Chaves E (2002) From continuum mechanics to fracture mechanics: the strong discontinuity approach. Engrg Fract Mech 69:113-136
12. Cazes F, Coret M, Combescure A, Gravouil A (2009) A thermodynamics method for the construction of a cohesive law from a nonlocal damage model. Int J Solids Structures 46: 1476-1490
13. Oliver J (1996) Modeling strong discontinuities in solid mechanics via strain softening constitutive equations, Part I: Fundamentals. Int J Numer Methods Eng 39:3575-3600

14. Moës N, Dolbow J, Belytschko T (1999) A finite element method for crack growth without remeshing. Int J Numer Methods Engrg 46:131-150
15. Armero F, Linder C (2009) Numerical simulation of dynamics fracture using finite elements with embedded discontinuities. Int J Fract 160:119-141
16. Hansbo A, Hansbo P (2004) A finite element method for the simulation of strong and weak discontinuities in solid mechanics. Comput Methods Appl Mech Engrg 193:3523-3540
17. Song JH, Areias PMA, Belytschko T (2006) A method for dynamic crack and shear band propagation with phantom nodes. Int J Numer Methods Engrg 67:868-893
18. Liu P, Bui TQ, Zhu D, Yu TT, Wang JW, Yin SH, Hirose S (2015) Buckling failure analysis of cracked functionally graded plates by a stabilized discrete shear gap extended 3-node triangular plate element. Compos Part B: Eng 77:179-193
19. Yu TT, Bui TQ, Liu P, Hirose S (2015) A stabilized discrete shear gap extended finite element for the analysis of cracked Reissner–Mindlin plate vibration problems involving distorted meshes. Int J Mech Mater Des 12:85-107.
20. Zeng Q, Liu Z, Xu D, Wang H, Zhuang Z (2016) Modeling arbitrary crack propagation in coupled shell/solid structures with XFEM. Int J Numer Methods Engrg 106:1018-1040
21. Englemann BE, Whirley RG, Goudreau GL (1989) A simple shell element formulation for large-scale elastoplastic analysis. In Analytical and Computational Models of Shells. Noor AL, Belytschko T, Simo JC Eds., CED-Vol. 3, ASME, New York, New York.
22. Hallquist JO (2006) LS-DYNA Theory Manual. Livermore Software Technology Corporation
23. Belytschko T, Lin JI, Tsay CS (1984) Explicit algorithms for the nonlinear dynamics of shells. Comput Methods Appl Mech Engrg 42:225-251
24. Dvorkin EN, Bathe KJ (1984) A continuum mechanics based four-node shell element for general non-linear analysis. Eng Comput 1:77–88
25. Simo JC, Hughes JC (1986) On the variational formulation of assumed strain methods. J Appl Mech 53:1685-1695
26. Bažant ZP, Planas J (1998) Fracture and Size Effect in Concrete and Other Quasibrittle Materials. CRC Press, Florida
27. Broumand P, Khoei, AR (2013) The extended finite element method for large deformation ductile fracture problems with a non-local damage-plasticity model. Engrg Fract Mech 112-113:97-125
28. Wu CT, Ma N, Takada K, Okada H (2016) A meshfree continuous-discontinuous approach for the ductile fracture modeling in explicit dynamics analysis. Comput Mech 58:391-409
29. Wu CT, Wu YC, Koishi M (2015) A strain-morphed nonlocal meshfree method for the regularized particle simulation of elastic-damage induced strain localization problems. Comput Mech 56:1039-1054
30. Guo Y, Wu CT, Hu W (2017), A Dynamic Ductile Failure Analysis of Shells Structures Using Extended Finite Element Method, Third China LS-DYNA User Conference, Shanghai
31. Wu CT, Ma N, Guo Y, Hu W, Takada K, Okada H, Saito K (2018) A dynamic ductile failure analysis of shell structures using a nonlocal XFEM method. Advances in Engineering Software, 123: 1-12
32. Guo Y, Wu CT (2018), An Enhancement of LS-DYNA XFEM Shells for Dynamic Ductile Failure Analysis, 15th International LS-DYNA Users Conference, Detroit